Catalysis Today 174 (2011) 59–64

Contents lists available at ScienceDirect

Catalysis Today

journal homepage: www.elsevier.com/locate/cattod

Catalytic dehydroxylation of glycerol to propylene glycol over Cu–ZnO/Al_2O_3 catalysts: Effects of catalyst preparation and deactivation

Suchart Panyad[a], Siriporn Jongpatiwut[a,b,*], Thammanoon Sreethawong[a,b],
Thirasak Rirksomboon[a,b], Somchai Osuwan[a,b]

[a] *The Petroleum and Petrochemical College, Chulalongkorn University, Soi Chula 12, Phyathai Road, Pathumwan, Bangkok 10330, Thailand*
[b] *Center for Petroleum, Petrochemicals, and Advanced Materials, Chulalongkorn University, Bangkok 10330, Thailand*

ARTICLE INFO

Article history:
Received 26 October 2010
Received in revised form 22 February 2011
Accepted 10 March 2011
Available online 9 April 2011

Keywords:
Dehydroxylation
Glycerol
Propylene glycol
Cu–ZnO/Al_2O_3
Incipient wetness impregnation
Co-precipitation
Sol–gel

ABSTRACT

The dehydroxylation of glycerol to propylene glycol was investigated over Cu–ZnO/Al_2O_3 catalysts prepared by three different methods—incipient wetness impregnation (IWI), co-precipitation (COP), and sol–gel (SG). The prepared catalysts were tested for their catalytic activity and selectivity in a continuous flow fixed-bed reactor at 523 K and 3.2 MPa under hydrogen atmosphere. The fresh and spent catalysts were characterized by several techniques, including BET, XRF, XRD, TPR, and TPO. Among the catalysts tested, the Cu–ZnO/Al_2O_3 catalyst prepared by the IWI method provided the highest catalytic performance, which could be due to its low coke formation. XRD, TPR, and TPO results indicated that possible causes of the catalyst deactivation are the combination of carbon deposit and sintering of active metals. Copper leaching was also found in the catalyst prepared by SG method.

© 2011 Elsevier B.V. All rights reserved.

1. Introduction

The availability of glycerol, a major by-product from biodiesel process, is predicted to exceed its demand in the near future as the biodiesel market grows rapidly [1,2]. The utilization of glycerol to produce other valuable chemicals becomes an interesting topic. One of the promising routes is the conversion of glycerol to propylene glycol (or 1,2-propanediol) by catalytic dehydroxylation. Propylene glycol is a commodity chemical used as a raw material in various applications, e.g. unsaturated polyester resins, functional fluids (such as anti-freezer, de-icing agent, and heat transfer media), pharmaceuticals, foods, cosmetics, liquid detergents, tobacco humectants, flavors and fragrances, personal care, paints, and animal feed [3,4].

The catalytic dehydroxylation (or hydrogenolysis) of glycerol to propylene glycol has been extensively studied in various aspects, including the development of catalysts [5–15], the development of reaction processes [6,16,17], and the reaction kinetics [18]. In recent studies, the reaction was investigated under moderate conditions in the presence of hydrogen and catalysts. Among the catalysts tested, Ru, Cu, and Ni-based catalysts exhibited high glycerol conversion and propylene glycol selectivity. Cu is superior to Ru and Ni catalysts due to its lower ability to cleave C–C bond in the glycerol molecule, resulting in lower undesired cracking products. Recent research works [8–10] demonstrated the high catalytic performance of Cu/ZnO-based catalysts in the dehydroxylation of glycerol to propylene glycol under mild conditions (473 K, 2.0 kPa). Glycerol conversion and propylene glycol selectivity varied with the Cu and ZnO particle sizes. Small ZnO and Cu domains gave positive effects on glycerol conversion and propylene glycol selectivity, respectively. High propylene glycol selectivity (92%) was achieved at 25% glycerol conversion. The addition of Al_2O_3 in Cu–ZnO catalyst was found to increase the catalyst stablitiy [19]. Recently, a kinetics study of the glycerol dehydroxylation over Cu–ZnO/Al_2O_3 was also determined [18]. The investigation suggested that the reaction over Cu–ZnO/Al_2O_3 take place via two consecutive steps, proposed by Dasari et al. [6], having acetol as the intermediate compound.

In the present work, the catalytic dehydroxylation of glycerol to propylene glycol was studied over the Cu–ZnO/Al_2O_3 catalysts prepared by three different methods—incipient wetness impregnation (IWI), co-precipitation (COP), and sol–gel (SG). The main purpose was to investigate the effect of catalyst preparation with an intention to improve the conversion of glycerol and selectivity

---

* Corresponding author at: The Petroleum and Petrochemical College, Chulalongkorn University, Soi Chula 12, Phyathai Road, Pathumwan, Bangkok 10330, Thailand. Tel.: +66 2 218 4139; fax: +66 2 215 4459.
E-mail address: siriporn.j@chula.ac.th (S. Jongpatiwut).

0920-5861/$ – see front matter © 2011 Elsevier B.V. All rights reserved.
doi:10.1016/j.cattod.2011.03.029

towards propylene glycol. In addition, the catalyst regeneration and deactivation were investigated.

2. Experimental

2.1. Materials and gases

Glycerol ($C_3H_5(OH)_3$, pharmaceutical grade, 99.99% purity) was obtained from PTT Chemical Public Company Limited, Thailand. Aluminum oxide (γ-Al_2O_3, extrudate with 99% purity) was provided by Saint-Gobain NorPro Corporation. Aluminum isopropoxide (AIP) ($Al(OCH(CH_3)_2)_3$, $\geq$98% purity) was obtained from Sigma–Aldrich. Aluminum (III) nitrate nonahydrate ($Al(NO_3)_3{\cdot}9H_2O$, $\geq$98% purity), copper (II) nitrate trihydrate ($Cu(NO_3)_2{\cdot}3H_2O$, lab grade $\geq$99% purity), zinc (II) nitrate ($Zn(NO_3)_2{\cdot}6H_2O$, reagent grade, 98% purity), nitric acid (HNO_3, 70%, v/v), and ethylene glycol ($C_2H_4(OH)_2$, reagent grade) were obtained from Ajax Finechem Pty Ltd. Ammonia solution (NH_3, 35 vol.%) was obtained from BDH Laboratory Supplies. Hydrogen (H_2, HP grade, 99.99% purity), helium (He, HP grade, 99.99% purity), nitrogen (N_2, HP grade, 99.99% purity), and air (HP grade, 99.99% purity) were supplied from Thai Industrial Gas Public Company Limited.

2.2. Catalyst preparation procedures

The Cu–ZnO/Al_2O_3 catalysts were prepared by three different methods—incipient wetness impregnation (IWI), co-precipitation (COP), and sol–gel (SG). For each technique, the desired amount of copper loading was 10 wt.% (maximum loading that does not form Cu bulk phase) and, the Cu:Zn molar ratio was kept at 1:4.

The Cu–ZnO/Al_2O_3 (IWI) catalyst was prepared using gamma alumina as the catalyst support. The as-received extrudate alumina was first ground and sieved to the size between 20 and 40 mesh (425–850 μm). Copper and zinc were impregnated into the alumina support with a mixed aqueous solution of copper nitrate and zinc nitrate. After the impregnation, the catalysts were dried at 383 K overnight and subsequently calcined at 773 K for 6 h.

The Cu–ZnO/Al_2O_3 (COP) catalyst was prepared using an aqueous solution containing desired amounts of copper nitrate, zinc nitrate, and aluminum nitrate. First, the mixture was stirred with a magnetic stirrer at room temperature. Then, ammonia solution was added dropwise to the mixture until pH of 7 was attained. After that, the excess solution was removed by filtration. The precipitate was washed repeatedly by distilled water, followed by drying at 383 K overnight and calcining at 773 K for 6 h. The obtained catalyst was palletized, ground, and finally sieved to the sizes between 425 and 850 μm.

Cu–ZnO/Al_2O_3 (SG) catalyst was prepared by the following steps. First, the AIP was ground and mixed with hot water at 353 K with the AIP-to-water molar ratio of 1:150. The mixture was stirred to disperse AIP overnight, and then desired amounts of copper nitrate, zinc nitrate, and ethylene glycol were added. After that, the mixture was continuously stirred for 1 h. Then, nitric acid/ammonia solution was added to accelerate the hydrolysis at the controlled solution pH of 10 to obtain the sol. After that, the sol was gradually evaporated at 353 K to get a dried gel before calcining at 773 K for 6 h. The obtained catalyst was pelletized, ground, and finally sieved to the sizes between 425 and 850 μm.

2.3. Catalyst characterization techniques

A nitrogen sorption system (Autosorb-1, Quantachrome) was employed to quantify the specific surface area and mean pore size distribution of the prepared catalysts. The Brunauer–Emmett–Teller (BET) method was used to determine the specific surface area. All the samples were outgassed under vacuum at 523 K for 6 h prior to the analysis to remove moisture and volatile substances on the catalyst surface. Temperature-programmed reduction (TPR) was employed to evaluate the reducible species present in the prepared catalysts and the suitable reduction temperatures. A 50 mg of each investigated catalyst was placed in a 4 mm I.D. quartz tube reactor, heated at a constant heating rate of 10 K/min in a flow of N_2 up to 423 K, and held at this temperature for 1 h in order to remove moisture from the catalyst surface. The sample was then cooled to room temperature before exposing to a flow of 5% H_2/Ar (10 mL/min). Then, the sample was heated to 1073 K with a constant heating rate of 10 K/min. The amount of hydrogen consumed was detected on-line by an SRI Model 110 TCD detector as a function of temperature. The crystalline structure of the catalysts was analyzed by a RINT-2200 Rigaku X-ray diffractometer (XRD), with a Cu tube for generating CuKα radiation (1.5406 Å) and a nickel filter. The analysis was conducted under the operating conditions of 40 kV and 30 mA. XRD patterns were measured in the 2θ range from 20° to 80° with a scanning rate of 5°/min. Temperature-programmed oxidation (TPO) was employed to analyze the amount and characteristics of coke deposited on the catalyst surface after the course of reaction. The oxidation of coke was performed in a 4 mm I.D. quartz tube reactor. A 30 mg of spent catalyst was placed in the reactor between two layers of quartz wool. The sample was purged at room temperature by flowing 2% O_2 in He for 30 min to stabilize the signal before ramping the temperature linearly to 1073 K (10 K/min). The CO_2/CO produced by the oxidation of the coke species was converted to methane using a methanator filled with 15% Ni/Al_2O_3 and operated at 673 K in the presence of H_2. The evolution of methane was analyzed by an FID detector. An X-ray fluorescence analyzer (XRF, WD-XRF PW-2400, Phillip) was used to analyze the elemental composition of the catalysts. An atomic absorption spectrometer (Varian SpectrAA 300) was used to determine the amount of Cu leached from the catalyst surface into the liquid products.

2.4. Catalytic activity measurements

The catalytic activity was examined using a 16 mm I.D. continuous flow fixed bed reactor made of stainless steel. In each test, a 2 g catalyst was placed in the center of reactor between layers of glass bead and glass wool. A thermocouple was inserted through a thermowell to measure and control the temperature of the catalyst bed. The catalyst was reduced at 673 K for 1 h in a hydrogen flow prior to the activity testing. After that, the reactor was cooled to the reaction temperature of 523 K, and the hydrogen pressure was adjusted to 3.2 MPa. An aqueous solution of 80 wt.% glycerol was continuously introduced to the reactor using a high pressure pump (Waters 515) along with a flow of hydrogen controlled by a mass flow controller (Brooks 5850E). The weight hourly space velocity (WHSV) was fixed at 2.8 h^{-1}. After the reaction, the product was trapped in a stainless steel cylinder immersed in an ice bath. The product obtained from the reaction was analyzed using a gas chromatograph (6890N Agilent) equipped with a Stabilwax® capillary column (0.53 mm × 30 m) and a flame ionization detector (FID).

After the first cycle of reaction, the spent catalyst was purged by a nitrogen flow before being regenerated in situ at 773 K with an air flow (10 mL/min). The temperature was slowly ramped with a heating rate of 5 K/min to 573, 673, 723, and 763 K by holding for 1 h at each step and 3 h at the last step. Then, the catalyst was cooled to room temperature and purged by a nitrogen flow before repeating the activity testing procedure in the same manner as the fresh catalyst. The regenerated catalysts were also analyzed to examine the causes of catalyst deactivation.

3. Results and discussion

3.1. Catalytic activity of fresh and regenerated catalysts

Prior to catalyst testing, blank tests with pure Al_2O_3, ZnO, and $ZnAl_2O_4$, were investigated under the identical catalyst testing conditions. No glycerol conversion was observed over the pure substrates. Therefore, conversion of glycerol observed over the catalysts is due to the incorporated copper. The plots of glycerol conversion, propylene glycol selectivity, and acetol selectivity as a function of time on stream over the Cu–ZnO/Al_2O_3 catalysts prepared by different methods (IWI, COP, and SG) are illustrated in Fig. 1a–c, respectively. The results show that all catalysts exhibited complete conversions at the beginning, then the conversions dropped considerably. This evidence indicates high catalytic activity but low stability of the catalysts. The major products observed in this study were propylene glycol and acetol with minute amounts of primary alcohols (methanol, ethanol, and propanol). The propylene glycol selectivity was high (>90%) and remained constant at high conversions. As the conversion decreased, the propylene glycol selectivity decreased with increasing acetol selectivity. These results agree well with the mechanism proposed by Dasari et al. [6] that propylene glycol is produced via two steps; (1) glycerol dehydration to acetol and (2) acetol hydrogenation to propylene glycol (see Scheme 1). The results also indicate the deactivation of both dehydration and hydrogenation sites simultaneously. Among the tested catalysts, the Cu–ZnO/Al_2O_3 (IWI) showed the highest stability as compared to the Cu –ZnO/Al_2O_3 (SG) and Cu–ZnO/Al_2O_3 (COP), respectively.

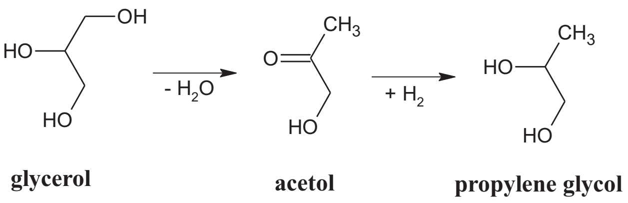

Scheme 1.

The spent Cu–ZnO/Al_2O_3 catalysts were regenerated in situ at 773 K in order to eliminate the deposited carbon on the surface. The regenerated catalysts were re-tested for their catalytic performances at the same conditions as were the fresh catalysts. Their catalytic performances in terms of glycerol conversion, propylene glycol selectivity, and acetol selectivity are shown in Fig. 2. The regenerated catalysts exhibited similar trends of conversions and selectivities as the fresh catalysts, in which the conversions reached 100% at the beginning of the reaction time and then dropped significantly. The regained complete conversion could be due to the highly active surface of the catalysts immediately after the regeneration process. The stability of the regenerated catalysts prepared by different methods was observed in the following order; IWI > SG > COP. However, the regenerated catalysts were much less stable than the fresh ones. For the IWI catalyst, the conversions started to drop at 15 h and 7 h TOS for the fresh and the regenerated catalysts, respectively. Similarly, the stable times (at 100% conver-

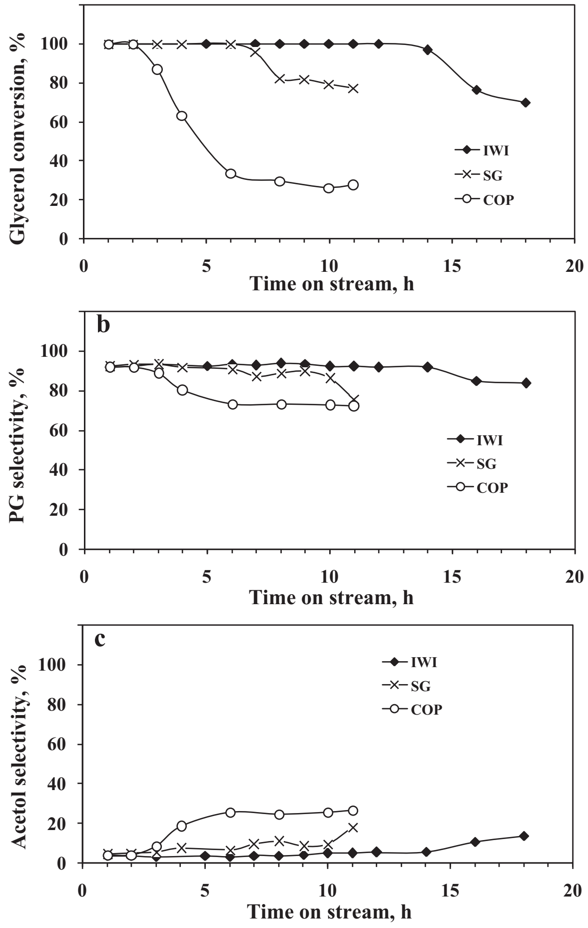

Fig. 1. Plots of (a) glycerol conversion, (b) propylene glycol selectivity, and (c) acetol selectivity as a function of time on stream over fresh Cu–ZnO/Al_2O_3 catalysts prepared by different methods (reaction conditions: 523 K, 3.2 MPa, H_2:glycerol = 4:1, and WHSV = 2.8 h^{-1}).

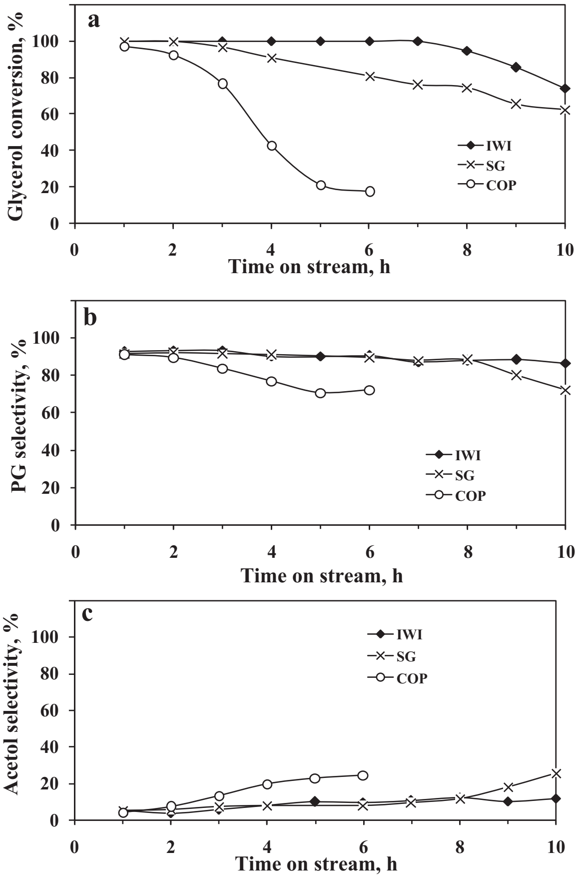

Fig. 2. Plots of (a) glycerol conversion, (b) propylene glycol selectivity, and (c) acetol selectivity as a function of time on stream over regenerated Cu–ZnO/Al_2O_3 catalysts prepared by different methods (reaction conditions: 523 K, 3.2 MPa, H_2:glycerol = 4:1, and WHSV = 2.8 h^{-1}).

Table 1
BET results of fresh and spent (after de-coking) Cu–ZnO/Al_2O_3 catalysts prepared by different methods.

Catalyst		BET surface area (m^2/g)	Pore volume (cm^3/g)	Pore diameter (nm)
IWI	Al_2O_3 support	256	0.834	8.94
	Fresh	145	0.477	8.91
	Spent (after de-coking)	129	0.357	8.94
SG	Fresh	175	0.395	6.18
	Spent (after de-coking)	146	0.369	8.90
COP	Fresh	182	0.185	3.64
	Spent (after de-coking)	128	0.144	4.64

sion) decreased from 7 to 2 h and from 2 to 1 h for the SG and COP catalysts, respectively. These results imply that the deactivation of the catalysts may not be solely due to the coke formation.

3.2. Characterization results and causes of catalyst deactivation

The fresh (calcined) and spent Cu–ZnO/Al_2O_3 (IWI), Cu–ZnO/Al_2O_3 (COP), and Cu–ZnO/Al_2O_3 (SG) catalysts were analyzed for their physical and chemical properties by several techniques, including BET, TPR, XRD, XRF, and TPO. For some techniques, the fresh (reduced) catalysts, spent (after de-coking) catalysts, and fresh (reduced/re-calcined) catalysts were also additionally investigated.

3.2.1. BET results

Table 1 shows the BET results of the fresh and spent (after de-coking) catalysts. For the Cu–ZnO/Al_2O_3 (IWI) catalyst, the BET surface area and pore volume were lower than those of the alumina support, while the pore diameter remained invariant. This loss of pore volume could be due to the high amount of metal loading [20]. The surface areas of the fresh Cu–ZnO/Al_2O_3 catalysts prepared by IWI, SG, and COP were 145, 175, 182 m^2/g, respectively. The relatively high surface area of catalysts prepared by SG and COP was also reported for a Ni/Al_2O_3 catalyst [21]. In terms of pore diameter, the Cu–ZnO/Al_2O_3 (IWI) catalyst showed the highest pore diameter (8.91 nm) as compared to SG (6.18 nm) and COP (3.64 nm) catalysts. These results point out the high surface areas with small pores of catalysts prepared by SG and COP. For all spent catalysts, the BET surface area and pore volume decreased while the pore diameter increased as compared to their corresponding fresh catalysts. These phenomena could be possibly due to the sintering of active metals or residual coke deposition which could plug the pore mouths, especially the small ones, during the course of reaction. This phenomenon was clearly observed for the Cu–ZnO/Al_2O_3 (COP) catalyst, which possesses relatively small pore diameter.

3.2.2. TPR results

The H_2-TPR profiles of the fresh (calcined) and spent (after de-coking) Cu–ZnO/Al_2O_3 catalysts are comparatively illustrated in Fig. 3. All of the fresh catalysts showed the reduction peaks at temperature below 623 K, indicating the reduction of highly dispersed copper oxide clusters on the catalysts, while the reduction of pure CuO used as a reference appeared at 667 K (data not shown). These results are in good agreement with the Cu–ZnO/Al_2O_3 prepared by co-precipitation investigated earlier in literatures [22,23]. The relatively higher reduction temperature with broader peaks of the catalysts prepared by SG and COP could be due to the strong metal–support interaction. The same behavior has been reported for Ni/Al_2O_3 catalysts prepared by SG and COP catalysts [21]. As clearly observed, a single reduction peak observed for the SG and COP catalysts indicated the homogeneous size distribution of copper oxide clusters on the catalysts. In contrast, the IWI catalyst exhibited a main reduction peak at 523 K with a shoulder at 543 K, indicating the presence of two different copper oxide species. This interpretation corresponds well with the XRD results, which will be discussed in the next section. Compared to the fresh catalysts, the reduction profiles of the spent catalysts (after de-coking) were partly shifted to a higher temperature. This shift could be possibly attributed to the sintering of active metals after the course of reaction [24]. Moreover, in the case of the Cu–ZnO/Al_2O_3 (SG) catalyst, not only the peak shift to a higher temperature, but also a significant decrease in the overall peak intensity was observed.

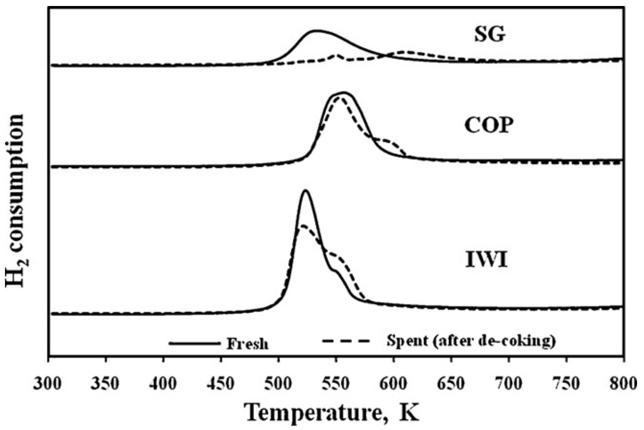

Fig. 3. TPR profiles of the fresh (calcined) and spent Cu–ZnO/Al_2O_3 (after de-coking) catalysts prepared by different methods.

Since the metal sintering during oxidation/reduction cycles is well established [19], the fresh Cu–ZnO/Al_2O_3 (IWI) was reduced, re-calcined, and then characterized by the TPR and XRD without passing the course of reaction in order to prove that the sintering observed in this work did not occur during the de-coking process. The TPR profiles of the fresh (calcined), spent (after de-coking), and re-calcined Cu–ZnO/Al_2O_3 (IWI) catalysts are shown in Fig. 4. The re-calcined catalyst exhibited a similar reduction profile as compared to the fresh catalyst. This demonstrates that the sintering of copper species occurred during the course of reaction instead of the de-coking which involved both oxidation and reduction steps.

3.2.3. XRD results

Fig. 5 shows the XRD patterns of the fresh (reduced) and spent Cu–ZnO/Al_2O_3 catalysts. For the fresh catalysts, the results show that zinc species exists in zinc oxide (ZnO) form for Cu–ZnO/Al_2O_3 (IWI) catalyst as the diffraction peaks at 2θ of 31.8°, 34.5°, and 36.3° were clearly observed. In contrast, broader peaks centered at 2θ of 31.0°, 36.4°, 44.5°, and 65.3° were detected on the Cu–ZnO/Al_2O_3 (SG) and Cu–ZnO/Al_2O_3 (COP), indicating the presence of zinc alu-

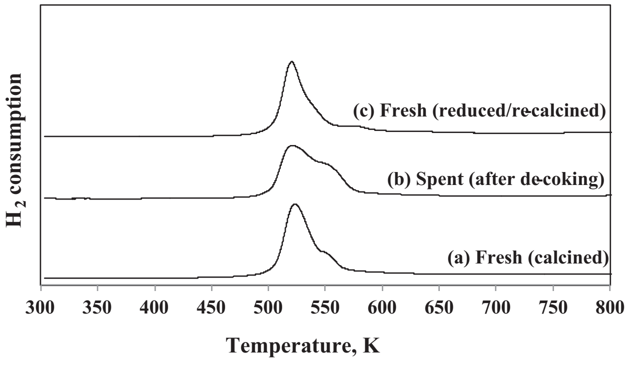

Fig. 4. TPR profiles of Cu–ZnO/Al_2O_3 (IWI) catalysts with different treatment procedures—(a) fresh (calcined), (b) spent (after de-coking), and (c) fresh (reduced/re-calcined).

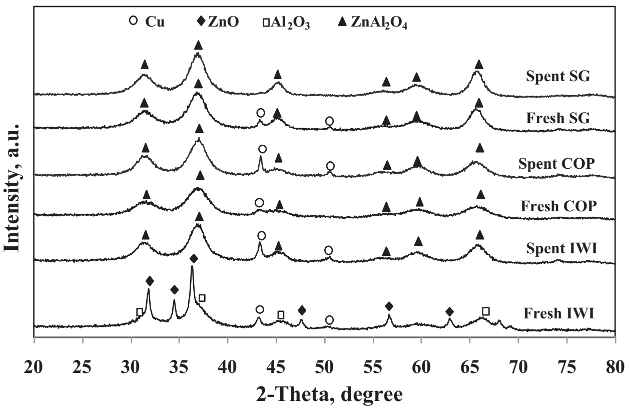

Fig. 5. XRD patterns of the fresh (reduced) and spent Cu–ZnO/Al_2O_3 catalysts prepared by different methods.

minate ($ZnAl_2O_4$) phase. The peak corresponding to metallic copper ($2\theta = 43.5$) of the fresh COP catalyst is relatively small as compared to the other two catalysts, implying that more highly dispersed copper particles are obtained on the SG catalyst surface.

A clear change in the XRD patterns was found for the spent IWI catalyst. The diffraction peaks of ZnO disappeared while the peaks corresponding to $ZnAl_2O_4$ were detected instead. This verifies the transformation of ZnO to $ZnAl_2O_4$ species during the course of reaction for the Cu–ZnO/Al_2O_3 (IWI) catalyst. The ZnO species may migrate from the upper layer of alumina support into the bulk and form $ZnAl_2O_4$. In addition, the spent Cu–ZnO/Al_2O_3 catalysts prepared by IWI and COP showed a relatively high intensity of Cu diffraction peak, as compared to the fresh catalysts. This implies the presence of a larger crystallize size of metallic Cu. In contrast, the Cu diffraction peak of the Cu–ZnO/Al_2O_3 (SG) catalyst decreased after the reaction. This result corresponds very well to the lower hydrogen uptake obtained from the TPR analysis (Fig. 3), suggesting the high possibility of Cu leaching from the catalyst surface during the reaction.

The XRD analyses of the fresh (calcined), fresh (re-calcined), and spent Cu–ZnO/Al_2O_3 (IWI) catalysts were also performed to evaluate the effect of oxidation/reduction cycles during the de-coking process and the results are illustrated in Fig. 6. The diffraction patterns of the fresh (calcined) and fresh (re-calcined) catalysts are almost identical, demonstrating that the de-coking process did not affect the structure of the catalyst. It can be deduced that reaction itself significantly affected the catalyst structure due to the phase change of ZnO and alumina to the spinel-like $ZnAl_2O_4$ phase.

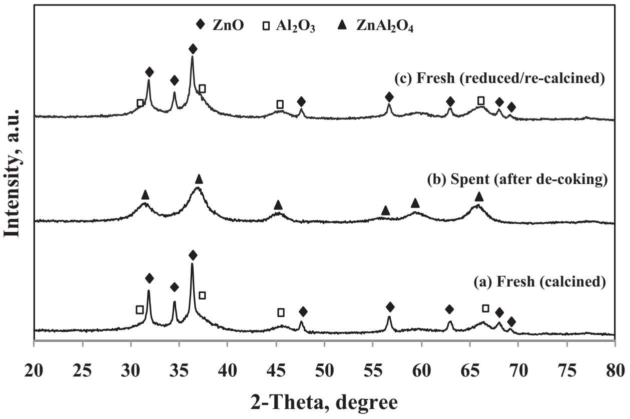

Fig. 6. XRD patterns of Cu–ZnO/Al_2O_3 (IWI) catalysts with different treatment procedures—(a) fresh (calcined), (b) spent (after de-coking), and (c) fresh (reduced/re-calcined).

Table 2
XRF results of fresh and spent (after de-coking) Cu–ZnO/Al_2O_3 catalysts prepared by different methods.

Catalyst		Composition (wt.%)		
		Cu	Zn	Al
IWI	Fresh	9.00	30.80	26.39
	Spent (after de-coking)	8.92	29.85	26.66
COP	Fresh	9.82	29.93	26.58
	Spent (after de-coking)	9.06	28.88	27.45
SG	Fresh	8.36	28.35	28.61
	Spent (after de-coking)	5.26	28.47	30.38

3.2.4. XRF and AAS results

The compositions of the fresh (calcined) and spent (after de-coking) catalysts prepared by different methods determined by XRF are summarized in Table 2. The Cu, Zn, and Al contents in the fresh and spent catalysts were comparable for both the Cu–ZnO/Al_2O_3 (IWI) and Cu–ZnO/Al_2O_3 (COP) catalysts, while the Cu content in the Cu–ZnO/Al_2O_3 (SG) was reduced significantly after the reaction. This result implies the loss of copper in Cu–ZnO/Al_2O_3 (SG) after the reaction, as also observed by the TPR and XRD analyses (Figs. 3 and 5).

To definitely confirm that the Cu species was leached from the Cu–ZnO/Al_2O_3 (SG) catalyst during the reaction, the obtained liquid product was analyzed for its copper contamination using AAS technique. As expected, the AAS results showed the presence of Cu species in the liquid product. The amounts of leached copper obtained from both the XRF and AAS analyses are similar (37 wt.% and 31 wt.%, respectively). These results verify that the Cu species was leached during the reaction under the tested conditions. Interestingly, although the leaching of Cu was observed in the Cu–ZnO/Al_2O_3 (SG) catalyst, its catalytic activity was greater than that of the Cu–ZnO/Al_2O_3 (COP) catalyst. These imply that both the coke formation and sintering of copper are the important causes of the catalyst deactivation while the leaching of copper exerts a minor effect.

3.2.5. TPO results

TPO profiles and calculated amounts of carbon deposition on the spent Cu–ZnO/Al_2O_3 catalysts are shown in Fig. 7. It was found that the spent COP catalyst contained the highest amount of coke (5.47 wt.%), compared to the spent SG (3.88 wt.%) and IWI (2.30 wt.%) catalysts. Not only found with high amount, but also the coke deposited on the COP and SG catalysts was also burnt out at relatively higher temperatures. This indicates high-molecular-weight coke species, which can be formed by undesired polymerization of unsaturated intermediates [25]. This result is consistent with the

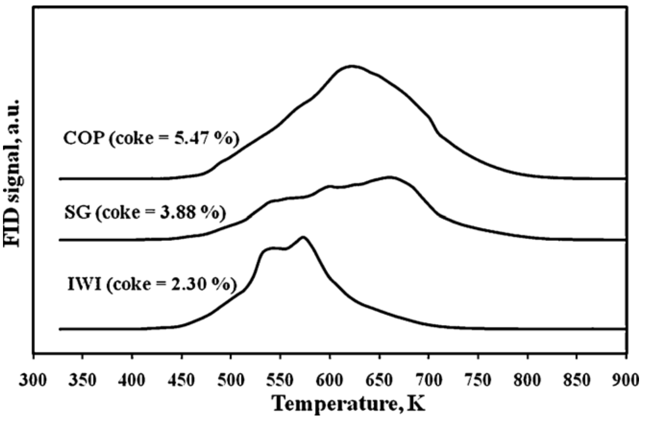

Fig. 7. TPO profiles of the spent Cu–ZnO/Al_2O_3 catalysts prepared by different methods.

faster deactivation of the Cu–ZnO/Al_2O_3 (COP) and Cu–ZnO/Al_2O_3 (SG) catalysts. However, as the sintering of active copper metal was also found during the reaction, the catalyst regeneration by a simple coke removal using heat treatment is not sufficient to regain the catalytic activity.

4. Conclusions

The Cu–ZnO/Al_2O_3 catalyst prepared by the IWI method exhibited the highest catalytic activity and stability as compared to the ones prepared by the SG and COP methods. The XRD, TPO and TPR results indicated that the causes of catalyst deactivation were the combination of coke formation and sintering of active copper metals. The Cu–ZnO/Al_2O_3 (SG) catalyst exhibited the lowest stability in terms of the highest Cu leaching. It was found that coke formation and sintering of Cu had more influence in suppressing the catalytic activity, compared to the Cu leaching.

Acknowledgments

The authors would like to acknowledge the Sustainable Petroleum and Petrochemicals Research Unit, Center for Petroleum, Petrochemicals, and Advanced Materials, Chulalongkorn University, Thailand; and the Petrochemical and Environmental Catalysis Research Unit under the Ratchadapisek Somphot Endowment Fund, Chulalongkorn University, Thailand.

References

[1] N. Rahmat, A.Z. Abdullah, A.R. Mohamed, Renew. Sustain. Energ. Rev. 14 (2010) 987–1000.
[2] S. Fernando, S. Adhikari, C. Chandrapal, N. Murali, Energy Fuel 20 (2006) 1727–1737.
[3] Available at http://www.dow.com/propyleneglycol/app/ (Access on February 20, 2011).
[4] J.A. Kenar, Lipid Technol. 19 (11) (2007) 249–253.
[5] J. Chaminand, L. Djakovitch, P. Gallezot, P. Marion, C. Pine, C. Rosier, Green. Chem. 6 (2004) 359–361.
[6] M.A. Dasari, P.-P. Kiatsimkul, W.R. Sutterlin, G.J. Suppes, Appl. Catal. A: Gen. 281 (2005) 225–231.
[7] J. Wang, S. Shen, B. Li, H. Lin, Y. Yuan, Chem. Lett. 38 (6) (2009) 572–573.
[8] L. Huang, Y.-L. Zhu, H.-Y. Zheng, Y.-W. Li, Z.-Y. Zeng, J. Chem. Technol. Biotechnol. 83 (2008) 1670–1675.
[9] S. Wang, H.C. Liu, Catal. Lett. 117 (2007) 62–67.
[10] M. Balaraju, V. Rekha, P.S. Sai Prasad, R.B.N. Prasad, N. Lingaiah, Catal. Lett. 126 (2008) 119–124.
[11] E.P. Maris, R.J. Davis, J. Catal. 249 (2007) 328–337.
[12] T. Miyazawa, S. Koso, K. Kunimori, K. Tomishige, Appl. Catal. A: Gen. 329 (2007) 30–35.
[13] J. Zhao, W. Yu, C. Chen, H. Miao, H. Ma, J. Xu, Catal. Lett. 134 (2010) 184–189.
[14] M. Balaraju, V. Rekha, P.S. Sai Prasad, B.L.A. Prabhavathi Devi, R.B.N. Prasad, N. Lingaiah, Appl. Catal. A: Gen. 354 (2009) 82–87.
[15] N.D. Kim, S. Oh, J.B. Joo, K.S. Jung, J. Yi, Korean J. Chem. Eng. 27 (2010) 431–434.
[16] E. D'Hondt, S.V.d. Vyver, B.F. Sels, P.A. Jacobs, Chem. Commun. 45 (2008) 6011–6012.
[17] D. Roy, B. Subramaniam, R.V. Chaudhari, Catal. Today 156 (2010) 31–37.
[18] Z. Zhou, X. Li, T. Zeng, W. Hong, Z. Cheng, W. Yuan, Chin. J. Chem. Eng. 18 (3) (2010) 384–390.
[19] M.S. Vaĭzquez, A.R. Rojas, V. Collins-Martıĭnez, A. Loĭpez Ortiz, Catal. Today 107–108 (2005) 831–837.
[20] L. Zhang, X. Wang, B. Tan, U.S. Ozkan, J. Mol. Catal. A: Chem. 297 (2009) 26–34.
[21] G. Li, L. Hu, J.M. Hill, Appl. Catal. A 301 (2006) 16–24.
[22] P. Kurr, I. Kasatkin, F. Girgsdies, A. Trunschk, R. Schlögl, T. Ressle, Appl. Catal. A: Gen. 348 (2008) 153–164.
[23] J.-P. Shen, C. Song, Catal. Today 77 (2002) 89–98.
[24] W. Dong-sheng, T. Yi-sheng, H. Yi-zhuo, T. Noritatsu, J. Fuel. Chem. Technol. 36 (2008) 171–175.
[25] G. Ertl, H. Knözinger, F. Schüth, J. Weitkamp, Handbook of Heterogeneous Catalysis, second ed., Wiley-VCH, Weinheim, 2008.